Available online at www.sciencedirect.com
SCIENCE DIRECT®
ELSEVIER
Journal of Constructional Steel Research 59 (2003) 47–61
JOURNAL OF CONSTRUCTIONAL STEEL RESEARCH
www.elsevier.com/locate/jcsr

Full-range stress–strain curves for stainless steel alloys

Kim J.R. Rasmussen *

Department of Civil Engineering, University of Sydney, Sydney, NSW 2006, Australia

Received 26 November 2001; accepted 13 February 2002

Abstract

The paper develops an expression for the stress–strain curves for stainless steel alloys which is valid over the full strain range. The expression is useful for the design and numerical modelling of stainless steel members and elements which reach stresses beyond the 0.2% proof stress in their ultimate limit state. In this stress range, current stress–strain curves based on the Ramberg–Osgood expression become seriously inaccurate principally because they are extrapolations of curve fits to stresses lower than the 0.2% proof stress. The extrapolation becomes particularly inaccurate for alloys with pronounced strain hardening.

The paper also develops expressions for determining the ultimate tensile strength (σ_u) and strain (ϵ_u) for given values of the Ramberg–Osgood parameters (E_0, $\sigma_{0.2}$, n). The expressions are compared with a wide range of experimental data and shown to be reasonably accurate for all structural classes of stainless steel alloys. Based on the expressions for σ_u and ϵ_u, it is possible to construct the entire stress–strain curve from the Ramberg–Osgood parameters (E_0, $\sigma_{0.2}$, n).

Keywords: Stainless steel; Stress–strain curves; Ramberg–Osgood curve; Tests

1. Introduction

Stainless steel alloys have low proportionality limits and extended strain-hardening capability. The pronounced yield plateau familiar from structural steel is nonexistent and so an equivalent yield stress is used in structural design, usually chosen as a

* Tel.: +61-2-9351-2125; fax: +61-2-9351-3343.
E-mail address: k.rasmussen@civil.usyd.edu.au (K.J.R. Rasmussen).

0143-974X/02/$ - see front matter
PII: S0143-974X(02)00018-4

suitable proof stress. The nonlinear stress–strain behaviour is acknowledged in the American [1], Australian [2] and South African [3] standards for cold-formed stainless steel structures which define the stress-strain curve in terms of the Ramberg–Osgood expression [4],

$$\varepsilon = \frac{\sigma}{E_0} + p\left(\frac{\sigma}{\sigma_p}\right)^n. \tag{1}$$

Eq. (1) was originally developed for aluminium alloys but has proven suitable for other nonlinear metals including stainless steel alloys. It involves the initial Young's modulus (E_0), the proof stress (σ_p) corresponding to the plastic strain p, and a parameter (n) which determines the sharpness of the knee of the stress–strain curve. In the design of aluminium and stainless steel structures, it has become industry practice to use the 0.2% proof stress ($\sigma_{0.2}$) as the equivalent yield stress. For this proof stress, the stress–strain relationship takes the form,

$$\varepsilon = \frac{\sigma}{E_0} + 0.002\left(\frac{\sigma}{\sigma_{0.2}}\right)^n. \tag{2}$$

It has also become standard practice to determine the parameter (n) using the 0.01% and 0.2% proof stresses which leads to the following expression,

$$n = \frac{\ln(20)}{\ln(\sigma_{0.2}/\sigma_{0.01})}. \tag{3}$$

Eq. (3) ensures that the Ramberg–Osgood approximation matches exactly the measured stress–strain curve at the 0.01% and 0.2% proof stresses. It generally provides close approximations to measured stress–strain curves for stresses *up to* the 0.2% proof stress.

In concentrically loaded columns, the strains are small when reaching the ultimate load for all practical ranges of length. It is therefore possible to base the design on the Ramberg-Osgood curve and achieve close agreement with experimental strengths, e.g. see [5,6]. This result was used [7] to develop a direct relationship between the column strength and the parameters n and e, where e is the nondimensional proof stress,

$$e = \frac{\sigma_{0.2}}{E_0}. \tag{4}$$

However, structural components which undergo significant straining before reaching their ultimate capacity, such as plates in compression or shear, compact beams failing by in-plane bending and tension members, may develop stresses beyond the 0.2% proof stress and strains well in excess of the 0.2% total strain,

$$\varepsilon_{0.2} = \frac{\sigma_{0.2}}{E_0} + 0.002. \tag{5}$$

When the strains exceed the 0.2% total strain ($\varepsilon_{0.2}$), the Ramberg–Osgood curve obtained on the basis of the 0.01% and 0.2% proof stresses may become seriously inaccurate, tending to produce too high stresses, as shown in Fig. 1. This particularly applies to alloys with low values of *n*. In this strain range, it is necessary to use a refined expression for the stress–strain curve with wider applicability range. This paper aims to develop such an expression within the following constraints:

1. Current values of *n*, such as those given in the American, Australian and South African standards for stainless steel structures, shall remain applicable. This implies that the stress–strain curve can be accurately determined using the Ramberg–Osgood expression for stresses up to the 0.2% proof stress.
2. In the stress range between the 0.2% proof stress and the ultimate tensile strength (σ_u), the stress–strain curve shall be defined in terms of a *minimum* of additional parameters.

These constraints ensure simplicity in the stress–strain curve formulation. It will be demonstrated that it is possible to obtain agreement with measured stress–strain curves within tolerances that would be deemed acceptable for a wide range of applications.

2. Recent approaches

MacDonald et al. [8] reported a series of tests on austenitic UNS30400 (AISI304) stainless steel channel columns. Ramberg–Osgood curves were fitted to stress–strain

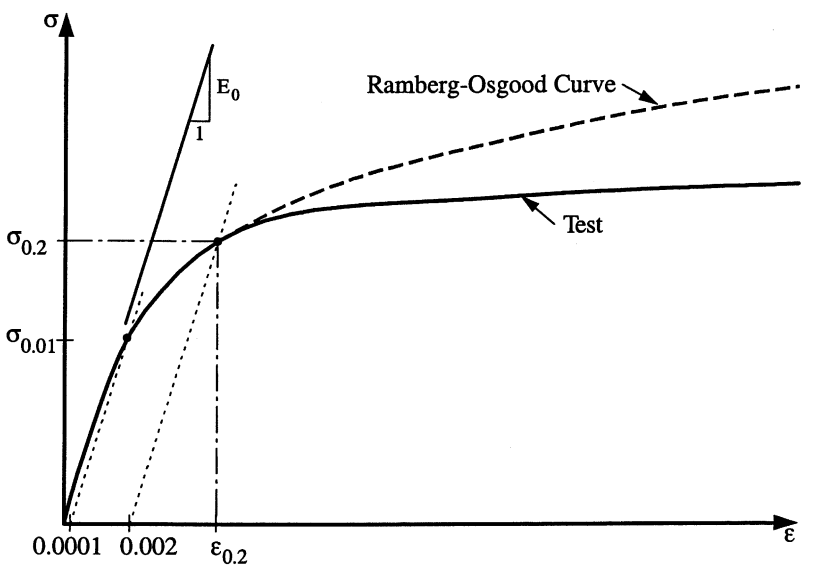

Fig. 1. Typical stress–strain curve for stainless steel and Ramberg–Osgood approximation.

curves obtained from stub column and tension coupon testing by using the 0.01% and 0.2% proof stresses to determine the *n*-parameter. The fitted Ramberg–Osgood curves were shown to err significantly at strains exceeding the 0.2% total strain ($\varepsilon_{0.2}$) and a modified expression was suggested in the form

$$\varepsilon = \frac{\sigma}{E_0} + 0.002\left(\frac{\sigma}{\sigma_1}\right)^{\left(i+j\left(\frac{\sigma}{\sigma_1}\right)^{k}\right)}. \tag{6}$$

where the constants *i*, *j* and *k* took values ranging from 2.5 to 6 depending on the thickness of the material tested. While this expression proved very accurate, it was limited in applicability to the particular alloy and thicknesses tested.

Olsson [9] studied advanced plasticity models for stainless steel alloys and performed a large number of tests on uniaxially and biaxially loaded coupons. He plotted the stress–strain curves as true stress (σ^t) vs engineering strain (ε) and observed experimentally that the stress–strain curve approached a straight line at large strains. He proposed that the true-stress vs engineering strain curve be approximated by a Ramberg–Osgood curve for strains up to a total strain of 2% and a straight line from this point onwards, as shown in Fig. 2. The straight line was chosen as an average fit to the measured stress–strain curve. It was not required to equal the true ultimate tensile strength (σ_u^t) at the ultimate total strain (ε_u).

Acknowledging the relationship between the true and engineering stresses,

$$\sigma^t = \sigma(1 + \varepsilon) \tag{7}$$

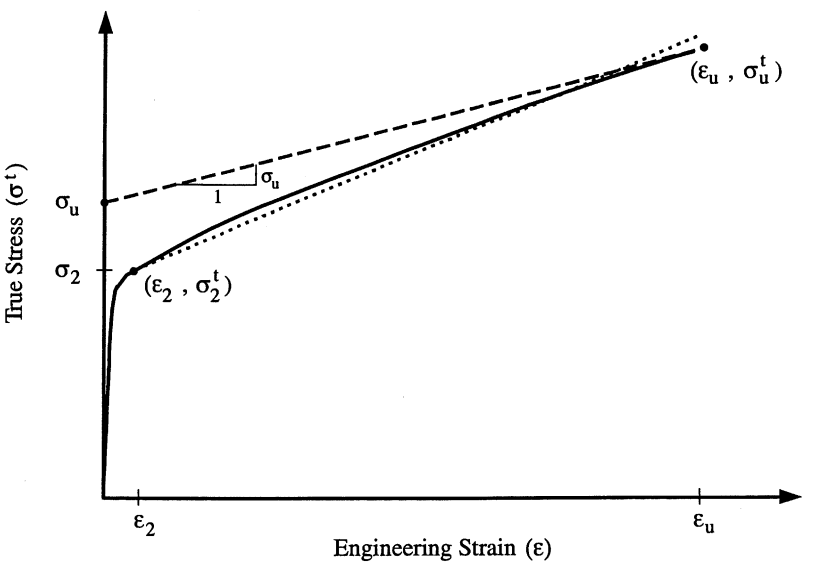

Fig. 2. Stress–strain curve in terms of true stress, and comparison with Olsson's model [9].

and observing that $d\sigma/d\varepsilon \to 0$ for $\sigma \to \sigma_u$, it is apparent that as $\sigma \to \sigma_u$ the true stress vs engineering strain curve asymptotes to the line,

$$\sigma^t = \sigma_u(1 + \varepsilon). \tag{8}$$

Evidently, the slope of this line and the intercept of the line with the stress axis both equal σ_u, as shown in Fig. 2. The slope of the line is different from the slope of the line through the true 2% proof stress and true ultimate tensile strength.

While Olsson's approach is attractive because of its theoretical justification, it lacks accuracy at small strains since it assumes the Ramberg–Osgood curve is valid for total strains up to 2%. Olsson determined the *n*-parameter by use of the 0.2% and 1% proof stresses which implies compromised accuracy in the important strain range $\varepsilon < \varepsilon_{0.2}$. In view of Constraint #1 stated in Section 1, Olsson's approach has not been adopted in this paper. However, it may prove appropriate for applications concerned mainly with large strains.

3. Test data

A wide range of tests has been used to develop the full-range stress–strain relation, including coupon tests on austenitic, duplex and ferritic stainless steel alloys. To cover the practical range of proof stress and *n*-values, the test data include coupons cut from annealed plate as well as cold-formed sections (rectangular hollow sections (RHS), circular hollow sections (CHS) and channels sections). The data are summarised in Table 1. Thirteen tests were performed on austenitic alloys (UNS30400, UNS30403, UNS31603), four on duplex alloys (UNS31803), and two on ferritic alloys (UNS43000, 3Cr12). The values of *n* range from 4.45 to 12.2, as shown in Table 1. The values of nondimensional proof stress ($e=\sigma_{0.2}/E_0$) range from 0.0014 to 0.0037.

Several references used for the experimental data did not include values of initial modulus (E_0) or proportionality stress ($\sigma_{0.01}$). In these cases, the values were determined from the stress–strain curves. In cases where the *n*-parameter was not presented, the value was calculated using Eq. (3).

4. Stress–strain curve expression

In view of Constraint #1 mentioned in Section 1, the stress–strain curve is chosen as a standard Ramberg–Osgood curve for stresses up to the 0.2% proof stress,

$$\varepsilon = \frac{\sigma}{E_0} + 0.002\left(\frac{\sigma}{\sigma_{0.2}}\right)^n \text{ for } \sigma \leq \sigma_{0.2}. \tag{9}$$

In developing a model for the part of the stress–strain curve between the 0.2% proof stress and the ultimate tensile strength (σ_u), it is noted that the stress–strain curve in this range is similar in shape to the initial part of the stress–strain curve up to the 0.2% proof stress, as shown in Fig. 3.

Table 1
Mechanical properties

Test	Alloy[a]	Reference[b]	Form[c]	E_0 (GPa)	$\sigma_{0.01}$ (MPa)	$\sigma_{0.2}$ (MPa)	σ_u (MPa)	ε_u	e	n	m[f]
1	UNS30400	[10]	RHS	188	314	612	780	0.40	0.0032	4.49	3.7
2	UNS30400	[10]	RHS	182	297	532	731	0.45	0.0029	5.14	3.5
3	UNS30400	[10]	RHS	190	178	312	635	0.65	0.0016	5.33	2.7
4	UNS30400	[10]	RHS	197	183	286	627	0.65	0.0015	6.71	2.6
5	UNS30400	[10]	RHS	190	241	402	661	0.55	0.0021	5.85	3.1
6	UNS30400	[10]	RHS	196	203	297	638	0.61	0.0015	7.87	2.6
7	UNS30400	[8]	Ch	180	241	460	695	0.34[e]	0.0026	4.66	3.3
8	UNS30400	[9]	P	190	215	327	611	0.57	0.0017	7.0	2.9
9	UNS30403	[5]	RHS	194	240	445	730[g]	0.51[g]	0.0023	4.85	3.1
10	UNS30403	[5]	RHS	190	240	470	730	0.51	0.0025	4.45	3.3
11	UNS30403	[5]	CHS	198	250	400	675[g]	0.51[g]	0.0020	6.37	3.1
12	UNS30403	[5]	CHS	198	250	400	675	0.51	0.0020	6.37	3.1
13	UNS31603	[9]	P	190	190	316	616	0.51	0.0017	5.88	2.8
14	UNS31803	[9]	P	190	526	699	878	0.32	0.0037	10.6	3.8
15	UNS31803	[11]	P	200	310	575	805	0.22	0.0029	4.85	3.5
16	UNS31803	[11]	P	215	430	635	820	0.22	0.0029	7.68	3.7
17	UNS31803	[11]	P	215	430	635	820	0.22	0.0029	7.68	3.7
18	UNS43000	[12]	P	200	200	320	622[d]	0.48[e]	0.0016	6.37	2.8
19	3Cr12	[12]	P	195	215	275	444[d]	0.38[e]	0.0014	12.2	3.2

[a] UNS30400~AISI304~ENV1.4301; UNS30403~AISI304L~ENV1.4306; UNS31603~AISI316L~ENV1.4436; UNS31803~ENV1.4462~Duplex 2205; UNS43000~AISI430~ENV1.4016; UNS41050~3Cr12~ENV1.4003.

[b] See reference list.

[c] RHS, rectangular hollow section; CHS, circular hollow section; Ch, channel section; P, plate or sheet.

[d] Ultimate tensile strength estimated using Eq. (20).

[e] Ultimate total strain estimated using Eq. (21).

[f] The parameter m is obtained using Eq. (17).

[g] Compression test. The values of σ_u and ε_u are assumed equal to the values for the corresponding tensile tests.

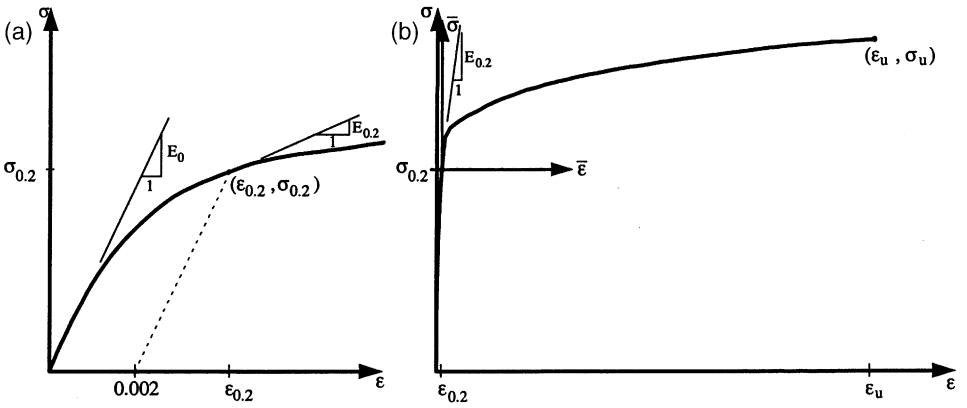

Fig. 3. Initial and full stress–strain curves. (a) Initial σ–ε curve, (b) full σ–ε curve.

This observation suggests a linear transformation of the stress and strain and the use of the Ramberg–Osgood expression (Eq. (1)) in the following form,

$$\bar{\varepsilon} = \frac{\bar{\sigma}}{E_{0.2}} + \bar{\varepsilon}_{u_p}\left(\frac{\bar{\sigma}}{\bar{\sigma}_u}\right)^m \text{ for } \sigma > \sigma_{0.2}. \tag{10}$$

where $\bar{\varepsilon}$ and $\bar{\sigma}$ are the transformed strain and stress (see Fig. 3b), defined as

$$\bar{\varepsilon} = \varepsilon - \varepsilon_{0.2} \tag{11}$$

$$\bar{\sigma} = \sigma - \sigma_{0.2} \tag{12}$$

The initial modulus to the curve ($E_{0.2}$) is also the tangent modulus of the stress–strain curve at the 0.2% proof stress, as shown in Fig. 3. By requiring continuity in slope at $\sigma_{0.2}$, $E_{0.2}$ is obtained from Eq. (9) as $d\sigma/d\varepsilon|_{\sigma = \sigma_{0.2}}$,

$$E_{0.2} = \frac{E_0}{1 + 0.002n/e} \tag{13}$$

In adopting Eq. (1), the "proof stress" (σ_p) is taken as the transformed ultimate tensile strength

$$\bar{\sigma}_u = \sigma_u - \sigma_{0.2} \tag{14}$$

and accordingly, the plastic strain (p) is the transformed ultimate plastic strain ($\bar{\varepsilon}_{u_p}$)

$$\bar{\varepsilon}_{u_p} = \varepsilon_u - \varepsilon_{0.2} - \sigma_u/E_0 \tag{15}$$

Stainless steel alloys are generally ductile and so negligible error is made by approximating the transformed ultimate plastic strain by the total ultimate strain,

$$\bar{\varepsilon}_{u_p} \approx \varepsilon_u \tag{16}$$

The exponent (m) is obtained by trial and error using the stress–strain curves reported

in the references summarised in footnote (b) of Table 1. Recognising that the exponent is dependent on the ultimate tensile strength in relation to the 0.2% proof stress, the following expression was obtained,

$$m = 1 + 3.5\frac{\sigma_{0.2}}{\sigma_u} \tag{17}$$

The full-range stress–strain curve can be written out in full as follows:

$$\varepsilon = \begin{cases} \dfrac{\sigma}{E_0} + 0.002\left(\dfrac{\sigma}{\sigma_{0.2}}\right)^n \text{ for } \sigma \leq \sigma_{0.2} \\ \dfrac{\sigma-\sigma_{0.2}}{E_{0.2}} + \varepsilon_u\left(\dfrac{\sigma-\sigma_{0.2}}{\sigma_u-\sigma_{0.2}}\right)^m + \varepsilon_{0.2} \text{ for } \sigma > \sigma_{0.2} \end{cases} \tag{18}$$

where $E_{0.2}$ and m are given by Eqs. (13) and (17), respectively. Figs. 4–6 show typical comparisons of the stress–stain curves obtained using Eq. (18) with experimental data for austenitic, duplex and ferritic alloys, respectively. The complete set of curves for the 19 tests listed in Table 1 are contained in Appendix A of [13].

The agreement between the test and proposed full-range stress–strain curves is generally excellent, while the Ramberg–Osgood curves extended past the 0.2% proof stress become increasingly inaccurate with strain, as shown in Figs. 4–6. The agreement is particularly good for the UNS30403 alloy, as shown in Fig. 4. The coupon test on UNS43000 alloy [12] was only reported for strains up to 0.007, as shown in Fig. 6. The agreement is good in this strain range. The agreement for the (duplex) UNS31803 is reasonable although the proposed curve is higher than the test curve

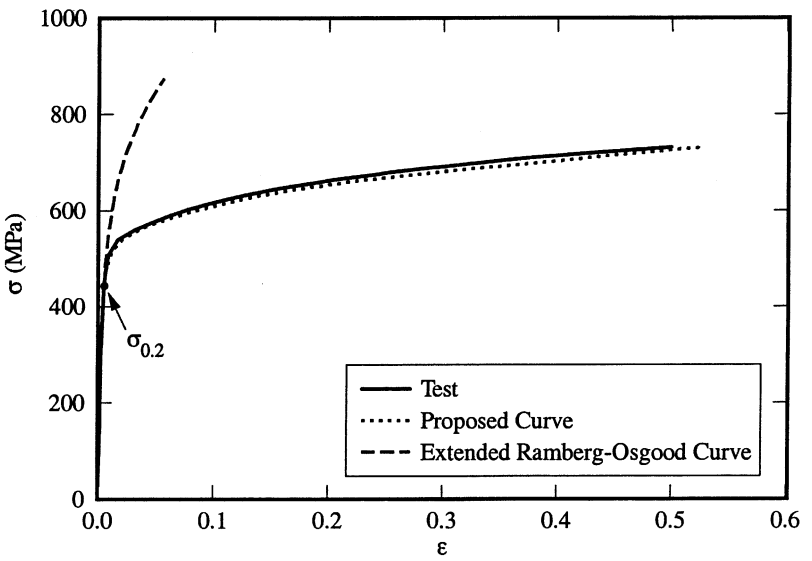

Fig. 4. Stress–strain curves for UNS30403 alloy. Test #9, see Table 1 for reference.

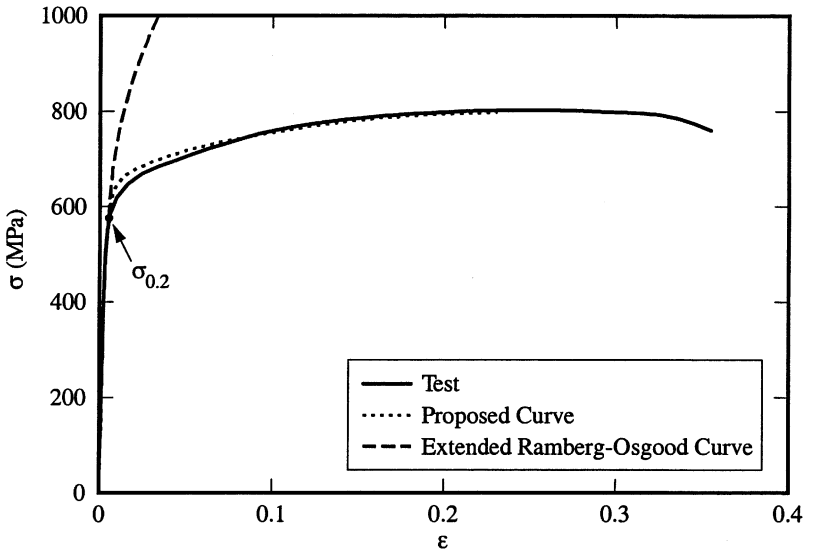

Fig. 5. Stress–strain curves for UNS31803 alloy. Test #15, see Table 1 for reference.

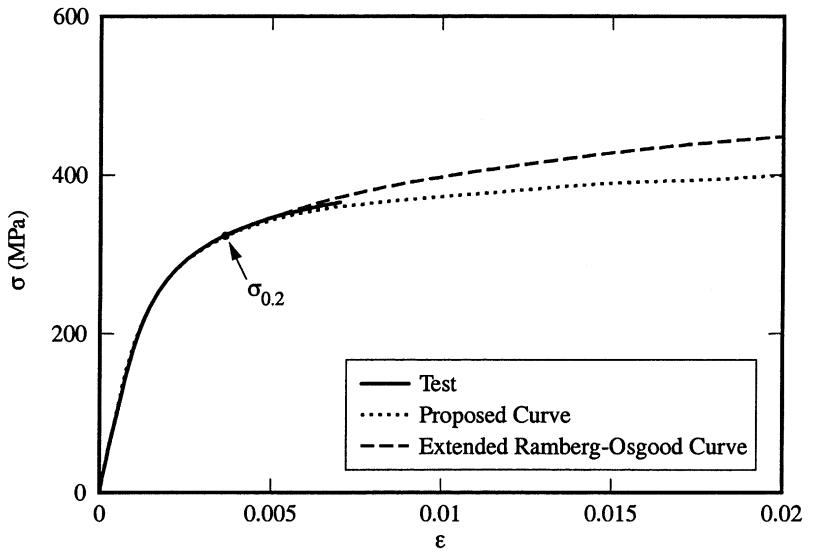

Fig. 6. Stress–strain curves for UNS43000 alloy. Test #18, see Table 1 for reference.

immediately after the 0.2% proof stress, as shown in Fig. 5. The discrepancy is a consequence of the slope ($E_{0.2}$) of the Ramberg–Osgood curve determined at the 0.2% proof stress which is too high.

5. Expressions for ε_u and σ_u

The expression for the full-range stress–strain curve (Eq. (18)) involves three parameters (E_0, n, $\sigma_{0.2}$) for $\sigma \leq \sigma_{0.2}$ and two additional parameters (ε_u, σ_u) for $\sigma > \sigma_{0.2}$. In many situations, the values of ε_u and σ_u may not be available or may not be achievable experimentally, as in the testing of compression coupons. To cater for these situations, equations are developed in this section for the determination of ε_u and σ_u in terms of n and e, where e is the nondimensional equivalent yield stress given by Eq. (4).

The experimental data are contained in Table 1, augmented by the results given in a report by the Steel Construction Institute [14] and reports by the Rand African University [15,16]. These reports do not contain complete stress–strain curves and could not be used for deriving a full-range expression for the stress–strain curves, as described in Section 4. The SCI report details 227 tension and compression coupon tests on austenitic (UNS30403, UNS31603) and duplex (UNS31803) alloys, while the South African reports detail tension and compression tests on ferritic UNS43000 stainless steel and weldable 12% chromium containing corrosion resisting steel, popularly know as 3Cr12, which is closely related to the ferritic alloy class. A total of 288 tests are contained in the South African reports for various thicknesses and direction of loading (longitudinal and transverse). Only the mean values of the results for each alloy, thickness and direction of loading have been used in this paper, adding a further 12 "tests" to the database. The British and South African experimental data are summarised in Appendix B of [13].

Evidently, the 0.2% proof stress approaches the ultimate tensile strength when increased by cold-forming, as is commonly found in austenitic alloys. This suggests that a relationship may exist between the ratio $\sigma_{0.2}/\sigma_u$ and the 0.2% proof stress. Accordingly, the ratio ($\sigma_{0.2}/\sigma_u$) is plotted against the nondimensional proof stress (e), as shown in Fig. 7. The graph indicates a linear relationship when excluding the ferritic alloys. A line of best fit through the test data for austenitic and duplex alloys produces the following equation,

$$\frac{\sigma_{0.2}}{\sigma_u} = 0.2 + 185e \text{ (austenitic and duplex alloys)} \tag{19}$$

The ferritic alloys (including 3Cr12) generally have larger n-values than austenitic and duplex alloys. Hence, their stress–strain curves have sharper knees which explain the higher values of ($\sigma_{0.2}/\sigma_u$) for given value of e, as shown in Fig. 7. To account for the influence of n, the following expression for $\sigma_{0.2}/\sigma_u$ has been obtained,

$$\frac{\sigma_{0.2}}{\sigma_u} = \frac{0.2 + 185e}{1 - 0.0375(n-5)} \text{ (all alloys)} \tag{20}$$

Fig. 8 shows the experimental values of ($\sigma_{0.2}/\sigma_u$) plotted against the approximate values given by Eq. (20). The data points are shown with solid markers and are not biased towards a particular alloy. However, they have greater scatter compared to the data points based on Eq. (19) which are shown with open markers in Fig. 8. Eq.

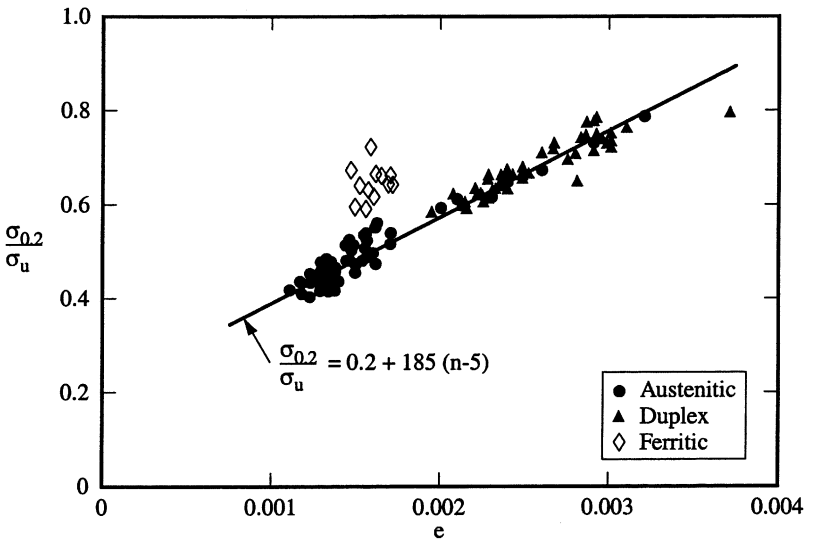

Fig. 7. $\sigma_{0.2}/\sigma_u$ vs e (the ferritic alloy test results are not included in the regression fit shown).

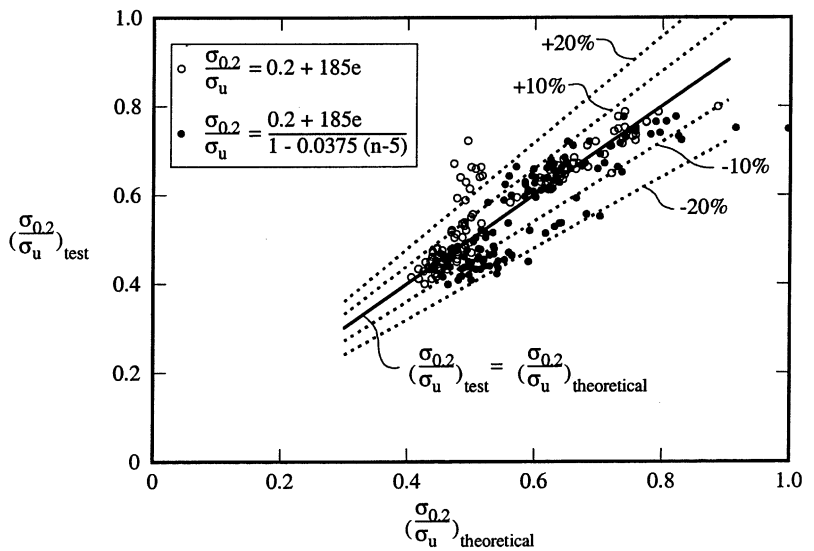

Fig. 8. $(\sigma_{0.2}/\sigma_u)_{test}$ vs $(\sigma_{0.2}/\sigma_u)_{theoretical}$.

(20) is therefore less accurate than Eq. (19) for austenitic and duplex alloys but is more generally applicable.

Finally, an expression is sought for determining the ultimate tensile total strain (ε_u). Recognising that $\varepsilon_u \to 0$ for $\sigma_{0.2} \to \sigma_u$, the ultimate tensile strain is plotted against the ratio of 0.2% proof stress to ultimate tensile strength, as shown in Fig. 9.

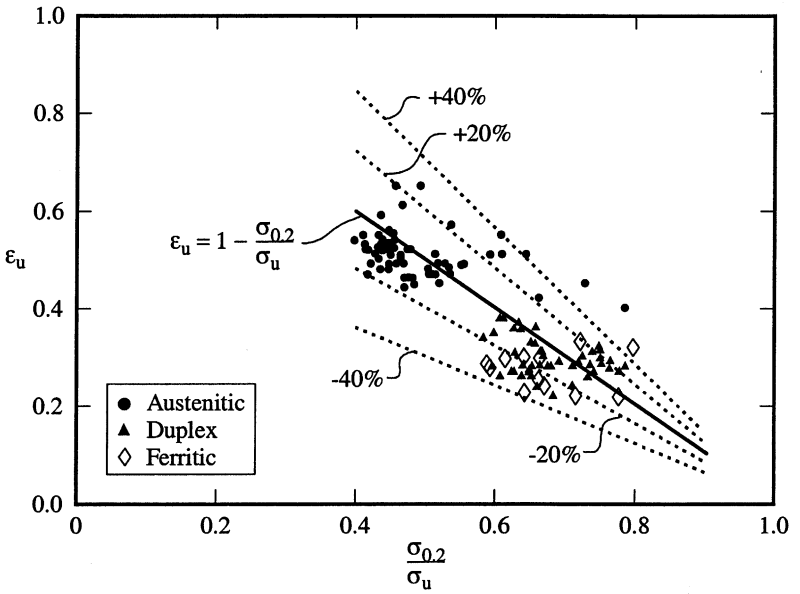

Fig. 9. ε_u vs ($\sigma_{0.2}/\sigma_u$).

There is significant scatter in the plot, as could be expected given the generally large variability in values of ultimate tensile strain. It is also not clear whether the ultimate tensile strain quoted in the references were the uniform elongation at the ultimate tensile strength, as has been assumed, or the total strain after fracture including local elongation in the area of necking.

The line of best fit can be closely approximated by,

$$\varepsilon_u = 1 - \frac{\sigma_{0.2}}{\sigma_u} \tag{21}$$

as shown with a solid line in Fig. 9. The data points are not biased towards a particular alloy and no attempt has been made to explore a possible relationship between ε_u and the n-parameter.

With Eqs. (20) and (21) at hand for determining σ_u and ε_u, the full-range stress–strain curves can be obtained from Eq. (18) for given values of E_0, $\sigma_{0.2}$ and n.

To assess the effect of the variability associated with Eqs. (20) and (21), stress–strain curves have been determined for the combinations of σ_u and ε_u shown in Tables 2 and 3 respectively. In all cases, the Ramberg–Osgood parameters were taken as E_0=200 GPa, $\sigma_{0.2}$=400 MPa, n=6, and the reference values of σ_u=675 MPa, ε_u=0.408 were determined using Eqs. (20) and (21). In Table 2, the ultimate tensile strength (σ_u) is changed by ±10% and ±20% while keeping ε_u=0.408 constant. Conversely, in Table 3, the ultimate tensile strain (ε_u) is changed by ±20% and ±40% while keeping σ_u=675 MPa constant. These changes in ultimate tensile strength and strain are representative of the largest differences between test data and the values

Table 2
Effect of change in σ_u

σ_u (MPa)	% change in σ_u	σ (ε=2%) (MPa)	% change in σ (ε=2%)
810	+20	513	+4.8
743	+10	502	+2.6
675	–	490	–
608	−10	474	−3.2
540	−20	455	−7.1

ε_u=0.408, E_0=200 GPa, $\sigma_{0.2}$=400 MPa, n=6.

Table 3
Effect of change in ε_u

ε_u	% change in ε_u	σ (ε=2%) (MPa)	% change in σ (ε=2%)
0.571	+40	481	−1.8
0.490	+20	485	−1.0
0.408	–	490	–
0.326	−20	496	+1.3
0.255	−40	502	+2.7

σ_u=675 MPa, E_0=200 GPa, $\sigma_{0.2}$=400 MPa, n=6.

of σ_u and ε_u determined using Eqs. (19) and (20), respectively, as shown in Figs. 8a and 9. The stress–strain curves resulting from the values of σ_u and ε_u given in Tables 2 and 3 are shown in Figs. 10a and 11, respectively.

The changes in stress at a strain of 2% are shown in the fourth columns of Tables 2 and 3. It follows from Table 2 that for the chosen values of (E_0, $\sigma_{0.2}$, n), a reduction of 20% in σ_u leads to a 7.1% decrease in σ (ε=2%). According to Table 3, a reduction of 40% in ε_u leads to a 2.7% increase in σ (ε=2%). Since these deviations in σ_u and ε_u represent the maximum deviations of the test data, it can be concluded that the expressions given by Eqs. (20) and (21) are likely to produce stress–strain curves with a maximum error of about 7% in stress at a strain of 2%, which for many applications is a likely upper bound to the ultimate limit state strains.

6. Conclusions

An expression has been derived (Eq. (18)) for the complete stress–strain curve for stainless steel alloys. The expression involves the conventional Ramberg–Osgood parameters (E_0, $\sigma_{0.2}$, n) as well as the ultimate tensile strength (σ_u) and strain (ε_u). It has been shown to produce stress–strain curves which are in good agreement with tests over the full range of strains up to the ultimate tensile strain.

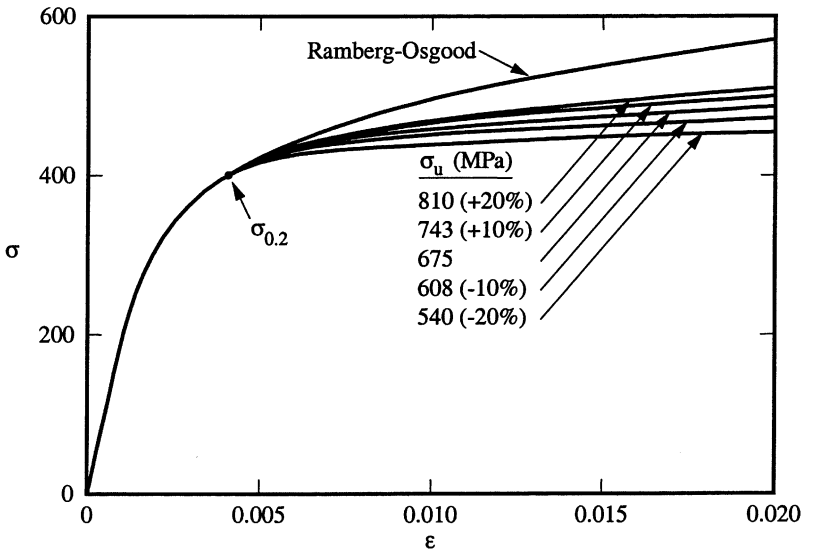

Fig. 10. Effect of change in σ_u.

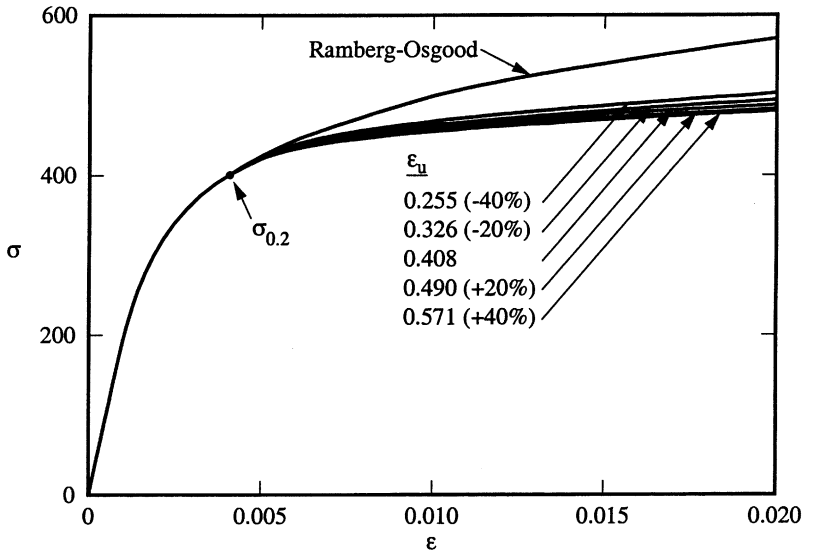

Fig. 11. Effect of change in ε_u.

Expressions are also derived for the ultimate tensile strength (σ_u) and strain (ε_u) in terms of the Ramberg–Osgood parameters; see Eqs. (20) and (21). The expressions are generally in reasonable agreement with experimental data. The maximum deviations observed are of the order of 20% for the ultimate tensile strength (σ_u) and 40% for the ultimate tensile strain (ε_u). It is shown that a deviation in σ_u of 20%

produces a maximum error in stress of 7.1% at a strain of 2% for a typical stainless steel alloy. Likewise, a deviation in ε_u of 40% produces a maximum error in stress of 2.7% at a strain of 2%. It can be concluded that the maximum variability associated with using Eqs. (20) and (21) leads to a maximum error on the stress of the order of 7% at a strain of 2%.

By using Eqs. (20) and (21) to determine (σ_u) and (ε_u), the full-range stress–strain curve can be obtained directly from the Ramberg–Osgood parameters (E_0, $\sigma_{0.2}$, n). This result is particularly useful for the design and numerical modelling of stainless steel structural members and elements where the stress–strain curve is specified in terms of the Ramberg–Osgood parameters, such as in the Australian, American and South African specifications for stainless steel structures.

References

[1] ASCE. Specification for cold-formed stainless steel structural members, ANSI/ASCE-8. New York: American Society of Civil Engineers; 1991.
[2] AS/NZS4673. Cold-formed stainless steel structures. Sydney: Standards Australia; 2001.
[3] SABS. Structural use of steel. Part 4: the design of cold-formed stainless steel structural members. Pretoria: The South African Bureau of Standards; 1997.
[4] Ramberg W, Osgood WR. Determination of stress–strain curves by three parameters. Technical note no. 503, National Advisory Committee on Aeronautics (NACA); 1941.
[5] Rasmussen KJR, Hancock GJ. Design of cold-formed stainless steel tubular members. I: Columns. Journal of Structural Engineering, ASCE 1993;119(8):2349–67.
[6] Rhodes J, MacDonald M, McNiff W. Buckling of stainless steel columns under concentric and eccentric loading. In: LaBoube RA, Yu W-W, editors. Proceedings, 15th International Specialty Conference on Cold-formed Steel Structures. University of Missouri-Rolla; 2000. p. 687–99.
[7] Rasmussen KJR, Rondal J. Strength curves for metal columns. Journal of Structural Engineering, ASCE 1997;123(6):721–8.
[8] MacDonald M, Rhodes J, Taylor GT. Mechanical properties of stainless steel lipped channels. In: LaBoube RA, Yu W-W, editors. Proceedings, 15th International Specialty Conference on Cold-formed Steel Structures. University of Missouri-Rolla; 2000. p. 673–86.
[9] Olsson A. Stainless steel plasticity—material modelling and structural applications. PhD thesis, Department of Civil and Mining Engineering, Luleå University of Technology, Sweden; 2001.
[10] Talja A, Salmi P. Design of stainless steel RHS beams, columns and beam–columns. VTT research note 1619, Technical Research Centre of Finland, Espoo; 1995.
[11] Burns T, Bezkorovainy P. Buckling of stiffened stainless steel plates. BE (Honours) thesis, Department of Civil Engineering, University of Sydney; 2001.
[12] Korvink SA, van den Berg GJ. Web crippling of stainless steel cold-formed beams. Proceedings, SSRC Annual Technical Session; 1993.
[13] Rasmussen KJR. Full-range stress–strain curves for stainless steel alloys. Research report no. R811, Department of Civil Engineering, University of Sydney; Nov 2001. Available at www.civil.usycl.edu.ou/publications.
[14] SCI. Tests on stainless steel materials. Report no. SCI-RT-251, Steel Construction Institute, London; 1991.
[15] Van der Merwe P, van den Berg GJ, Marshall, V. Experimental stress–strain curves for cold-rolled 3Cr12 steel sheets. Internal Report no. MD-21, Department of Civil Engineering, Rand Afrikaans University, July 1986.
[16] Van der Merwe P, van den Berg GJ. Experimental stress–strain curves for cold-rolled type 430 steel sheets. Internal report no. MD-36, Department of Civil Engineering, Rand Afrikaans University; August 1987.